Published in final edited form as:
Brain Stimul. 2014 ; 7(5): 748–756. doi:10.1016/j.brs.2014.06.011.

Focused Ultrasound-mediated Non-invasive Brain Stimulation: Examination of Sonication Parameters

Hyungmin Kim[a,b,c], **Alan Chiu**[a], **Stephanie D. Lee**[a], **Krisztina Fischer**[a], and **Seung-Schik Yoo**[a]

[a]Department of Radiology, Brigham and Women's Hospital, Harvard Medical School, 75 Francis Street, Boston, MA 02115, USA

[b]Department of Mechanical Engineering, Korea University, Anam-dong, Sungbuk-gu, Seoul 136-713, Korea

[c]Department of Radiology, Incheon St. Mary's Hospital, College of Medicine, The Catholic University of Korea, 56 Dongsu-ro, Bupyeong-Gu, Incheon 403-720, Korea

Abstract

Background—Transcranial focused ultrasound (FUS) has emerged as a new brain stimulation modality. The range of sonication parameters for successful brain stimulation warrants further investigation.

Objective—The objective of this study was to examine the range of FUS sonication parameters that minimize the acoustic intensity/energy deposition while successfully stimulating the motor brain area in Sprague-Dawley rats.

Methods—We transcranially administered FUS to the somatomotor area of the rat brain and measured the acoustic intensity that caused excitatory effects with respect to different pulsing parameters (tone-burst duration, pulse-repetition frequency, duty cycle, and sonication duration) at 350 and 650 kHz of fundamental frequency.

Results—We observed that motor responses were elicited at minimum threshold acoustic intensities (4.9–5.6 W/cm^2 in spatial-peak pulse-average intensity; 2.5–2.8 W/cm^2 in spatial-peak temporal-average intensity) in a limited range of sonication parameters, *i.e.* 1–5 ms of tone-burst duration, 50% of duty cycle, and 300 ms of sonication duration, at 350 kHz fundamental frequency. We also found that the pulsed sonication elicited motor responses at lower acoustic intensities than its equivalent continuous sonication.

Corresponding Author: Seung-Schik Yoo, Ph.D. MBA, Department of Radiology, Brigham and Women's Hospital, Harvard Medical School, 75 Francis Street, Boston, MA 02115, Tel: +1 617-732-9464, Fax: +1 617-732-9185, yoo@bwh.harvard.edu.

Conclusion—Our results suggest that the pulsed application of FUS selectively stimulates specific brain areas-of-interest at an acoustic intensity that is compatible with regulatory safety limits on biological tissue, thus allowing for potential applications in neurotherapeutics.

Keywords

focused ultrasound; sonication; neuromodulation; parameter; neurostimulation

Introduction

Brain stimulation methods, such as transcranial magnetic stimulation (TMS) (1) or direct current stimulation (DCS) (2), allow for non-invasive evaluation and modulation of the brain function. These non-invasive techniques contributed to the expansion of our knowledge about the brain by probing spatiotemporal characteristics of specific neural substrates. However, the lack of spatial specificity and penetration depth due to the inductive nature of magnetic stimulation (in the case of TMS) or electrical current conduction in *in vivo* tissue (for DCS) leaves margins for substantial improvement. Recent developments in optogenetic brain stimulation method (3) provide superior spatial specificity compared to other brain stimulation methods; however, they require cell-level genetic alterations to express light-activated ion channels as well as invasive procedures to introduce the light source to the specific brain anatomy, preventing its immediate application to a widespread human study.

The demand for methods enabling non-invasive brain stimulation with superior spatial specificity and penetration depth, therefore, has been warranted, and focused ultrasound (FUS) has emerged as a new modality that shows exceptional promise in the field of brain stimulation and subsequent functional brain mapping. FUS typically utilizes a single (4) or multiple ultrasound transducers that are actuated independently (5–6) to deliver highly-localized acoustic energy to a specific focal location-of-interest. Using a lower acoustic frequency (<1 MHz) than those used for diagnostic imaging (on the order of 1–15 MHz), FUS can be administered through the intact skull in a focal manner (6–8). FUS-based brain stimulation may provide several distinct advantages over other brain stimulation methods. It allows for spatial specificity (on the order of a few millimeters, depending on the fundamental frequency and transducer configuration) and superior penetration depth without requiring invasive surgical procedures or genetic alterations.

The neuromodulatory potentials of FUS were suggested by the pioneering work of Fry and colleagues (9), which demonstrated that FUS administered to the lateral geniculate nuclei of the thalamus reversibly inhibited the visual pathway in cats. These potentials were further seen by monitoring electroencephalography (EEG) recordings in cats, which demonstrated attenuated seizure activity (10). The application of FUS to excised rodent hippocampal tissue was also shown to enhance or suppress electrically-evoked neural field potentials (11–12). Recently, studies on intact rodent and rabbit brain tissue confirmed the excitatory and suppressive neuromodulatory properties of FUS for not only the central nervous system but also the peripheral nervous system (13–15). Several research groups have also reported that the modulation of neural activity is feasible through the application of short bursts of ultrasound pulses (14–18), demonstrated by using a wide range of pulsing schemes having

variations in duty cycle (DC), tone-burst duration (TBD), pulse-repetition frequency (PRF), sonication duration (SD), acoustic intensity (AI), and fundamental frequency (FF). On the other hand, continuous ultrasound waves have also been shown to modulate the brain neural activities (9, 19–21); however, the question remains as to which one is more effective in achieving the desired modulation.

For the safe use of ultrasound in brain stimulation, using the lowest possible acoustic intensities (represented by spatial-peak pulse-average intensity - I_{sppa} and spatial-peak time-average intensity - I_{spta} [W/cm^2]) and energy density (E_{sppa} [J/cm^2]) (22) is desired to prevent unwanted mechanical or thermal damage to the tissues during and after the sonication. To our knowledge, there are a few systematic investigations that probed the efficacy of ultrasound sonication over various combinations of pulsing parameters, including a comparison with continuous US sonication (18, 23). In the present study, we were motivated to examine FUS sonication parameters that would minimize the AIs to elicit successful brain stimulation and associated motor responses in Sprague-Dawley rats. We measured the threshold I_{sppa} (associated with the degree of acoustic pressure) and I_{spta} (indicating the rate of energy deposition in the tissue) using various combinations of discretized pulsing parameters. The pulsing scheme, which elicited motor responses at the lowest AIs among the tested parameters, was compared to continuous sonication that had an equivalent amount of acoustic energy deposition.

Methods and Materials

Animal preparation

All animal experiments described in this study were approved by the Harvard Medical Area Standing Committee on Animals. The Sprague-Dawley rat (all male, n=37) was anesthetized using an intraperitoneal injection of a 80:10 mg/kg, ketamine/xylazine mixture. After a sufficient level of anesthesia was achieved, the rat scalp was depilated with household razor blades. As shown in Figure 1a, the rat was then positioned, using ear bars and a teeth holder, on a fixation frame (SRP-AR, Narishige, Japan) that can be moved in all directions using a 3-axes mechanical platform. The FUS transducer was immersed in a cone-shaped plastic bag containing degassed water, and the bag was positioned over the rat’s head. The bag containing the degassed water uses the water as the media that acoustically couples the transducer to the skull. The degassing process is required to minimize the absorption and distortion of acoustic pressure waves in the water bag. Hydrogel (Aquasonic, Parker Laboratories, Fairfield, NJ, USA) was also applied to promote the acoustic coupling between the scalp and the water bag.

Sonication setup and characterization of FUS transducer

The schematics of the sonication control system and data acquisition for the detection of the tail motor responses are described in Figure 1b, with an illustration of sonication parameters in Figure 1c. The bursts of pulsed waves, each sinusoidal, were generated using two serially connected arbitrary function generators (33210A, Agilent, Santa Clara, CA), whereby the first function generator (FG1 in Fig. 1b) controlled the PRF, SD and inter-stimulus interval (ISI) by triggering the operation of the second FG (FG2 in Fig. 1b), which controlled the

ultrasound FF, TBD and AI. For continuous mode sonication, a single function generator (FG2 in Fig. 1b) was used to control the FF, SD, AI and ISI. For both pulsed and continuous sonication modes, a fixed ISI of 2 s was adopted. The corresponding duty cycle (DC), which is the percentage of sonication that is active compared to the continuous sonication (*i.e.* DC of 100 %), can be described as the product of TBD (in ms) and PRF (in kHz) as a percentage value.

The generated sinusoidal waves were then amplified by a linear power amplifier (240L, ENI Inc., Rochester, NY) before being transmitted to the FUS transducer. Two air-backed, spherical segment FUS transducers (6 cm in diameter, 7 cm in radius-of-curvature, each operating at the 350 or 650 kHz FF) were used. The acoustic pressure field at the focus generated by the transducer was measured in a rubber-laid, degassed water tank using a needle-type hydrophone (HNR500, Onda, Sunnyvale, CA) attached to the 3-axes robotic platform (Bi-Slides, Velmex, Bloomfield, NY). The location of the focal plane perpendicular to the incident acoustic beam path, 7cm radius-of-curvature away from the transducer surface, was first estimated using the time delay between the actuation of the transducer and the detection of the pressure wave (DSO-X 2012A, Agilent Technologies, Santa Clara, CA). The acoustic pressure was then measured in a space spanning 2.5 × 2.5 cm^2 with 0.5 mm steps in the transversal plane, and 7 × 3 cm^2 with 0.5 mm steps in the longitudinal plane relative to the sonication path. The I_{sppa} was estimated by dividing the pulse intensity integral (PII) by the pulse duration in compliance with the American Institute of Ultrasound Medicine (AIUM) standards (24), resulting in the equation $A^2/2\rho c$, whereby A is the peak pressure, ρ is the density of the medium (1000 kg/m^3), and c is the speed of sound in the medium (1480 m/s) (25), and the I_{spta} was calculated by multiplying the pulse duty cycle to the I_{sppa}. The corresponding duty cycle (DC), which is the percentage of sonication that is active compared to the continuous sonication (*i.e.* DC of 100 %), can be described as the product of TBD (in ms) and PRF (in kHz) as a percentage value. The resulting acoustic focus, defined at the full-width-at-half-maximum (FWHM) of the normalized acoustic intensity profile on the focal plane, was roughly cigar-shaped (6.5 mm in diameter, 24 mm in length for 350 kHz; 3.5 mm in diameter, 15 mm in length for 650 kHz; Figure 2). The degree of acoustic pressure attenuation through the rat skull at 350 and 650 kHz FFs was measured using freshly-isolated *ex vivo* rat skulls (n=5). The averaged pressure attenuation across the five rat skulls was 12.1±2.3% for 350 kHz FF and 16.8±2.1% for 650 kHz FF. Factoring in the pressure attenuation through the rat skull, the relationship between the transducer input voltage to the output AIs at the focal area was established up to 28 W/cm^2 I_{sppa} in both transducers.

Excitation of the brain somatomotor area and detection of the corresponding motor responses

Previous investigations revealed that a light state of anesthesia is conducive to inducing ultrasound-mediated motor responses in rodents ((23),(26),(27)). Guided by this information, we performed the experiments under a light anesthetic state, and used the onset of irregular and rapid respiratory motions from the rats (28) as a distinctive physiological cue to initiate application of the ultrasound. Among the various somatomotor cortical areas that could be stimulated by sonication (*e.g.* causing whisker or limb movements),

stimulation of the tail somatomotor area was selected since the resulting tail motion can be readily detected *via* visual inspection and a motion sensor (Piezoelectric Pulse Transducer, MLT1-1010/D, AD Instruments, CO) (29). In some of the previous studies, EMG had been adopted to detect peripheral motor responses induced by FUS stimulation (18, 23). EMG captures subtle corticospinal motor responses elicited by stimulating the somatomotor area of the brain; however, the resulting EMG signals are often confounded by spontaneous muscle activities, requiring further corrections to determine the success rates and latencies from the stimulus onset (23). Since we aimed to measure the presence of the muscle recruitment and motion that are manifested by the stimulation of motor neural units in the brain, we selected the actual muscle movement caused by cortical stimulation as a measure of a successful stimulus outcome. The aim is also in line with a recent observation that ultrasound-mediated neural simulation is an all-or-nothing event and not correlated with the magnitude of the EMG signal (23). Referencing the functional atlas obtained by transdural electrical stimulation on the motor cortex of the rat (30), the somatomotor area of the brain that elicits tail movement was located (midline, 2 mm posterior to the Bregma). The location of the sonication focus was guided to the area-of-interest using the visual guidance system presented in our previous work (31), and adjusted further by maneuvering the 3-axes platform within a 2 mm distance from the initial location.

Overview of sonication trials

The criterion for a successful stimulation was the detection of sonication-synchronized tail motions (each stimulus sonication was given in two second intervals) that occurred consecutively for five times. The threshold AI that elicited stimulation-related motor responses was determined for different combinations of the sonication parameters. Initially, we used a set of sonication parameters (0.5 ms TBD, 1 kHz PRF, 300 ms SD, 10 W/cm^2 I_{sppa}), which has been previously shown to stimulate somatomotor areas in rats (29). An ISI of 3 s was used to allow for enough time gaps between the stimulations. Once the tail movement was successfully elicited, the sonication parameters were then adjusted to the specific parameters-of-interest (Table 1). AIs were subsequently reduced down to 4 W/cm^2 I_{sppa} and incrementally increased about 10% of the preceding I_{sppa} for each step until the criterion for the presence of tail movement was achieved. The criterion was 3 times the standard deviation from the baseline (non-excitation state) signal as detected by the motion sensor. The sequence of sonication trials, employing a different set of sonication parameters for each trial, was randomized and balanced across the animals to minimize the potential confounding effects due to the anesthesia level (23, 26). After determining the threshold AI, another set of test sonication trials were given below and above the threshold to confirm the finding.

Sonication parameters

The sonication parameters tested are listed in Table 1. A 350 kHz transducer was initially used due to its superior stimulation efficiency over the 650 kHz transducer (18, 23). The threshold AIs that elicited the motor responses were examined over the range of TBDs (0.25, 0.5, 1, 2, 3, and 5 ms) using three different pulse DC groups (n=11, 279±23 g for 50% DC; n=9, 286±36 g for 30% DC; n=10, 290±21 g for 70% DC) at a fixed SD of 300 ms, whereby the use of 50% DC elicited motor responses at the lowest AIs (see Results section;

Figure 3). Then, while maintaining the 50% DC, we conducted experiments on an additional group of animals to determine the threshold AIs in two additional SD conditions (n=9, 297±35 g for 200 ms SD, n=9, 297±38 g for 400 ms SD). The use of 300 ms SD showed the lowest threshold in terms of both AIs and E_{sppa} for eliciting successful tail motion (see Result section; Figure 4). Using 50% DC and 300 ms SD, the threshold AIs that elicited the movement responses were subsequently examined at 650 kHz FF across a different set of animals (n=8, 289±12 g) to examine the stimulation efficiency compared to the use of 350 kHz FF. We also used continuous sonication to measure the threshold AIs that generated motor responses (n=9, 297±12 g), whereby the SD was adjusted to 150 ms, depositing the same overall acoustic energy as the pulsed sonication (50% DC, 300 ms SD). Repeated sonication sessions were allowed on the same animal, but with different sonication parameter sets. A minimum gap of 2 days was maintained between the sessions. There was no significant difference in animal weights between any of the groups compared (Table 2). The method of statistical analysis is provided in the Supplement.

Examination of potential thermal effects

To examine the potential thermal effects from the sonication, we estimated the acoustic intensity that would elevate the tissue temperature by 1°C. To do so, we used the formula $\Delta T = 2\alpha It/\rho_b C_p$; where α = the absorption coefficient (0.05 cm^{-1} at 350 kHz), I = the intensity of ultrasound in the focal region, t = the ultrasound pulse duration, ρ_b = the density of brain tissue, and C_p = the specific heat of the brain tissue, whereby $\rho_b C_p$ is 3.796 $J \cdot cm^{-3} \cdot °C^{-1}$ (32–33). We found that an I_{sppa} of at least 189 W/cm^2 would be necessary for the set of sonication parameters that has the highest rate of energy deposition (*i.e.* 70% DC, 300ms SD) at 350kHz FF. On the other hands, the acoustic intensity level corresponding to the allowed Mechanical Index for diagnostic ultrasound device (*i.e.* 1.9 (34) according to the FDA-guideline) was 43 W/cm^2 I_{sppa} at 350 kHz.

Histological assessment

All experimental animals were allowed to survive for different periods of time (n=11, 0–6 days; n=18, 7–14 days; n=8, 15–26 days) after the sonication to monitor any adverse acute and long-term biological effects associated with the procedure. Immediately after sacrificing the animal, systemic transcardial circulation of 10% formalin was applied to fix the brain tissue. The skull was then extracted and immersed in 10% formalin for an additional 1–2 weeks before the brain tissue was extracted for histological assessment (n=30). Serial sections were applied perpendicularly to the sonication path along the cortex and hippocampus, and stained with hematoxylin and eosin (H&E) to examine the presence of hemorrhaging or tissue damage.

Results

FUS-mediated tail movement

The nature of the tail movement was oscillatory, which occurred only upon each FUS stimulation event (the motion returned back to neutral position, the motion data as shown in Fig. 1a). Occasional elicitation of the movement from the hind leg or whiskers that accompanied the tail movement, which has been observed elsewhere (27), was also detected

due to proximity of functional areas between tail and hind leg; however, was not included in the analysis due to lack of objective measurement of the motion characteristics.

Comparison among different duty cycles at 350 kHz FF employing 300 ms SD

The results pertaining to the group-averaged threshold AIs across the six tone-burst durations for the three different duty cycles (30, 50, and 70%) in the case of sonication employing 300ms SD at 350 kHz FF are shown in Figure 3. In terms of I_{sppa} (Figure 3a), significant differences were observed among the three different DCs across all TBDs (one-way ANOVA; $p<0.05$). A subsequent Tukey-Kramer *post-hoc* analysis revealed that there was a significant difference (shown as a bracket in the Figure 3) between 30% and 50% DC for all TBDs, and between 30% DC and 70% DC across all TBDs, except 1 ms TBD. No significant difference was observed between 50% DC and 70% DC for any of the TBDs. On the other hand, in terms of I_{spta} (Figure 3b), there were significant differences among the three different DCs for 1–5 ms TBDs (one-way ANOVA; $p<0.05$). A Tukey-Kramer *post-hoc* analysis showed that there were significant differences between 30% and 70% DC only for 1 ms TBD, and between 50% and 70% DC for 1–5 ms TBDs. No significant differences were observed between 30% DC and 50% DC for any of the TBDs. In summary, the data suggests that the use of 50% DC elicited motor responses at lower AIs, favoring its use in terms of a lower I_{sppa} (compared to the use of 30% DC) as well as a lower I_{spta} (compared to the use of 70% DC), for the range of 1–5 ms TBDs.

Comparison between each pair of tone-burst durations within a group

A set of pair-wise comparisons (paired t-test; two-tailed) for the minimum AIs capable of eliciting tail movement was conducted between each pair of TBDs, across the three DCs (Supplementary Table A1). In 30% DC, the minimum threshold AIs were observed at 1 ms TBD (9.34±1.2 W/cm^2 I_{sppa}, 2.8±0.36 W/cm^2 I_{spta}). There were significant differences in AIs between 1 ms and the other TBDs, except for the 2 ms TBD. In 50% DC, the minimum threshold AIs were observed at 2 ms TBD (4.91±0.46 W/cm^2 I_{sppa}, 2.45±0.23 W/cm^2 I_{spta}), in which the threshold AIs showed significant differences when compared with those of 0.25 and 0.5 ms TBDs. In 70% DC, the minimum threshold AIs were observed at 0.5 ms TBD (5.78±1.04 W/cm^2 I_{sppa}, 4.04±0.73 W/cm^2 I_{spta}), where the threshold AIs only exhibited significant differences when compared with those at 0.25 and 5 ms TBDs.

Comparison among different sonication durations using 50% DC

The group-averaged threshold AIs and E_{sppa}, plotted against the six TBDs across the three SDs are shown in Figure 4. Significant differences in threshold AIs and E_{sppa} among the three SDs were observed across all TBDs (one-way ANOVA). A subsequent Tukey-Kramer *post-hoc* analysis showed that there were significant differences in AIs (both I_{sppa} and I_{spta}) between 200 and 300 ms SD for all TBDs, and between 200 and 400 ms SD for 0.5 ms TBD, and between 300 and 400 ms SD for 1 and 2 ms TBDs (Figure 4a). On the other hand, from the perspective of E_{sppa}, significant differences existed between 300 and 400 ms SD across all TBDs, and between 200 and 300 ms SD for 1 and 2 ms TBDs (Figure 4b). In summary, the use of 300 ms SD elicited motor responses at lower threshold AIs and E_{sppa} than the other tested SDs (200 and 400 ms) for 1 and 2 ms TBDs.

Comparison among different fundamental frequencies using 50% DC and 300 ms SD

The results pertaining to the group-averaged threshold AIs when comparing the two fundamental frequencies (350 and 650 kHz FFs) are shown in Figure 5. There were significant differences in the threshold AIs and E_{sppa} between 350 and 650 kHz FFs for all TBDs (one-tailed t-test; $p<0.05$), whereby the use of 350 kHz FF elicited stimulatory motor responses at lower threshold AIs and E_{sppa} than the use of 650 kHz FF.

Comparison between pulsed and continuous sonication

The comparison between the pulsed sonication (50% DC, 300 ms SD, 350 kHz FF) and its equivalent continuous sonication (150 ms SD, 350 kHz FF) showed that the continuous sonication was able to elicit tail movement in rats at 7.73±0.83 W/cm^2 I_{sppa} (I_{spta} equates to I_{sppa} due to the use of 100% DC), and 1.16±0.12 J/cm^2 E_{sppa}. Significant differences between pulsed and continuous sonication existed in the range of 0.5–5 ms TBDs in terms of I_{sppa} and E_{sppa} (one-tailed t-test, Supplementary Table A2), and for all TBDs in terms of I_{spta} (one-tailed t-test, Supplementary Table A2). These values were much greater when compared to the minimum values observed when using pulsed sonication at 2 ms TBD (*i.e.* 4.91±0.46 W/cm^2 I_{sppa}, 2.45±0.23 W/cm^2 I_{spta}, and 0.74±0.07 J/cm$_2$ E_{sppa}). However, this distinction disappears at 0.25 ms TBD, *i.e.*, no significant differences in I_{sppa} and E_{sppa} were observed between pulsed and continuous sonication. The results suggest that pulsed sonication elicits motor responses at lower AIs and E_{sppa} than its equivalent continuous sonication for the range of 0.5–5 ms TBDs (mean difference values are shown in Supplementary Table A2). The latency between the application of the FUS and the initiation of the tail movement was 208±57 ms in case of the pulsed sonication (50% DC and 300 ms SD), whereas the latency was slightly reduced to 167±78 ms (two-tailed t-test, p=0.04) in case of the continuous sonication (150 ms SD) with the equivalent overall energy deposition.

Post-sonication histological assessment

Histological analysis based on H&E staining did not show the presence of any tissue damage or hemorrhage associated with the sonication (example shown in Figure 6a). One animal, however, that was exposed to a high AI (22.4 W/cm^2 I_{sppa}; 11.2 W/cm^2 I_{spta}) and high mechanical index (MI) of 1.38 for a short period of time (3 ISIs, *i.e.* < 9 s using 1 ms TBD, 50% DC and 300 ms SD) during testing later exhibited several areas containing hemosiderin, which indicated the potential of local bleeding (arrow in Figure 6b).

Discussion

In this study, by testing various combinations of pulsed sonication parameters, we derived pulsed sonication parameters that stimulate brain somatomotor areas and, subsequently elicit motor responses at the lowest acoustic intensities (both I_{sppa} and I_{spta}). Among the tested parameters, the use of 1–5 ms TBD, 50% DC, 300 ms SD, and 350 kHz FF was deemed to be effective by manifesting stimulation at the lowest possible AIs and energy deposition. The use of continuous sonication, which was designed to deliver equivalent acoustic energy as the pulsed sonication, elicited motor responses at higher AIs compared to those of its pulsed counterpart.

Effects of duty cycle, tone-burst duration, and sonication duration

We observed that the use of 50% and 70% DC elicited stimulation-mediated motor responses at a lower I_{sppa} than 30% DC across most of the TBDs tested (Figure 3a). On the other hand, in terms of I_{spta} (Figure 3b), the use of 50% DC elicited motor responses at a lower I_{spta} than the use of 70% DC for 1–5 ms TBDs. These findings indicate that the use of an intermediate DC of 50% stimulates the somatomotor area at lower, overall AIs compared to the use of 30% and 70% DC. In terms of the use of different TBD under each DC (as also shown in Figure 3), the minimum threshold AIs were observed at 2 ms TBD in the case of 50% DC. For example, at 2 ms TBD, motor responses were observed at 4.91±0.46 W/cm^2 I_{sppa} and 2.45±0.23 W/cm^2 I_{spta}. However, there were no significant differences in threshold AIs between 2 ms TBD and the other TBDs used (*i.e.* 1, 3, and 5 ms TBDs), except for 0.25 and 0.5 ms TBDs (Supplementary Table A1). This indicates that the use of a lower TBD (less than 1 ms) significantly increased the threshold AIs compared to the rest of the tested TBDs. According to the parabolic curves describing the threshold AIs shown in Figure 3, there was rather a steep increase in AIs when short TBDs, *i.e.*, 0.25 and 0.5 ms, were used. For example, the use of 0.25 ms TBD elicited motor responses at 6.73±0.56 W/cm^2 I_{sppa}, 3.36±0.28 W/cm^2 I_{spta}, and 1.01±0.08 J/cm^2 E_{sppa}. Therefore, the use of intermediate TBDs, on the range of 1–5 ms, operating at 50% DC, would provide the desired brain stimulation at the lowest AIs, serving as an effective pulsing scheme.

The presence of particular sonication parameters that elicit stimulatory effects at a lower acoustic intensity than other parameters can potentially be explained by the Neuronal Bilayer Sonophore (NBLS) model (35) that addresses the mechanism of neuronal excitation under the exposure of an acoustic pressure field. According to the model, ultrasound pressure waves induce mechano-electrical effects in the neural cell membrane, and subsequently produce neural excitation, primarily though the changes of membrane capacitance as well as transmembrane ion currents. The use of different pulsing schemes (for example, the use of different TBDs at the same duty cycle) may impose a differential mechanical impact on the piezoelectric properties of the cell membranes as well as voltage-dependent membrane potentials, thus possibly contributing to the parabolic features of the threshold curves identified in this study. For example, the model suggested that an optimal choice of duty cycle may exist for ultrasound-mediated neural stimulation through non-linear interactions between charge accumulation across the membrane and one of voltage-dependent sodium channels. It is also interesting to note that 400 ms SD sonication, although its first 300ms duration was as same as the 300 ms condition, required a higher I_{sppa} for eliciting the tail movement. We conjecture that the longer sonication durations might have recruited inhibitory neural circuits that ended up raising the threshold. The examination of the possibility for recruitment of inhibitory neural cells (such as interneurons (36)), along with the validation of the NBLS model in the context of *in vivo* setting, is needed to elucidate the mechanism behind the acoustic neural stimulation.

Pulsed versus continuous sonication and the effects of fundamental frequency

We found that a pulsing scheme provides superior stimulation efficiency (*i.e.*, stimulation occurred at lower AIs) compared to the continuous sonication. Continuous sonication, which was designed to deposit the same amount of acoustic energy as the pulsed sonication (50%

DC, 300 ms SD, 350 kHz FF), elicited tail movement, but at much higher AIs than its equivalent pulsed sonication across most of the TBDs, except for the shortest TBD tested (*i.e.* 0.25 ms; see Supplementary Table A2). Our results are in agreement with recent bio-piezoelectric modeling of membrane capacitance and successful induction of neural cell firing due to the ultrasound pulsation (35), which showed that pulsing scheme may lead to higher stimulation efficiency than continuous sonication. In regards to the comparison of two FFs, the use of 350 kHz FF elicited stimulatory motor responses at a lower threshold I_{sppa} and I_{spta} than the use of 650 kHz FF (Figure 5). The results comparing the use of 350 and 650 kHz FFs agreed with previous studies (18, 23), which showed that the use of a lower FF is favored for eliciting motor responses in mice using collimated ultrasound sonication on the brain.

In terms of *in vivo* testing, our findings are congruent with the findings by King and colleagues (23), whereby a TBD of 0.2 ms would require a higher I_{sppa} and E_{sppa} than its equivalent continuous sonication based on the extrapolation of the threshold curves (Figure 3). However, this agreement seems to apply only to the use of a short TBD, whereas the continuous sonication to the somatomotor area of the brain elicited motor responses more frequently than its pulsed sonication counterpart in their study (23). The present study, which examines much wider ranges of pulsing parameters (*i.e.* various tone-burst durations, sonication durations, and duty cycles) compared to the study by King and colleagues (23), showed that the pulsing scheme provides superior stimulation efficiency (*i.e.*, stimulation occurred at lower AIs) compared to that of the continuous, single-pulse sonication. However, the discrepancies in the experimental design, *e.g.* transducer type (non-focused vs. focused), animal model (mice vs. rat), and efficacy metrics (success rate vs. threshold acoustic intensity), warrant further investigations.

Stimulation of the tail motor cortex induced by the FUS in the present study was assessed as an all-or-nothing event based on the tail twitching as manifested by the muscle recruitment. Similarly, the detection of body parts and the quantification of the success rate of stimulation has also been adopted by other groups to assess the efficacy of ultrasound stimulation of the corresponding brain area (23, 27); however, it is important to note that overall excitability and functionalities of the brain circuitries are the outcome of the intricate and non-linear interactions among neural substrates, which covers a much wider scope beyond the dichotic stimulatory events. Therefore, further investigation is needed on non-linear neural responses due to neuromodulatory FUS, including the examination of the suppressive effects by the pulsed application of FUS to the brain (13–14).

Biological safety of FUS sonication

In this study, we were able to elicit motor responses at less than 3 W/cm^2 I_{spta} (corresponding to 6 W/cm^2 I_{sppa}, peak pressure of 0.42 MPa, MI of 0.71) by using the effective sonication parameters described above. An AI of 3 W/cm^2 I_{spta} complies with the upper limit of ultrasound physiotherapy equipment set by the IEC (International Electrotechnical Commission) standard (34). According to the histological assessment, we did not observe any tissue damage or hemorrhage associated with the sonication except in one animal that was once exposed to a relatively high AI (22.4 W/cm^2 I_{sppa}; 11.2 W/cm^2

I_{spta}). The corresponding peak pressure (0.81 MPa) was still far below the threshold of the cavitation-related brain tissue damage in the absence of air bubbles (40 MPa) (37). Other than the H&E staining presented in here, a more detailed histochemistry examination focusing on inflammatory cells, for example, astrocytes and microglia (38), would be necessary to probe the presence of less visible perturbations resulting from the sonication. Long-term EEG monitoring along with other motor evaluation tasks after the sonication would also be conducive to revealing the potential functional changes that may not have been histologically evident.

Conclusions

We examined a range of FUS sonication parameters that stimulated the motor cortex of rats *in vivo* and found there were 'sweet-spot' parameters that elicited neural activation with minimal acoustic energy deposition to the biological tissues. This result is conducive to determining the bio-compatible pulsing parameters for functional brain mapping using FUS, which will confer non-invasive means for probing the region-specific brain functions. Furthermore, the differential neuromodulatory capability of FUS would incite a new generation of treatments for various neurological and psychiatric disorders.

Supplementary Material

Refer to Web version on PubMed Central for supplementary material.

Acknowledgments

This work was supported by grants from the National Research Foundation of Korea (Korean Ministry of Education, Science and Technology, 2010-0027294 to Kim), the Korea Institute of Science and Technology Institutional Program (2E23031 to Yoo), and National Institute of Health (R21 NS074124 to Yoo; partial salary supports for the staffs). The authors thank Dr. Shinsuk Park for his intellectual contributions in data analysis.

List of Abbreviations

TBD	Tone-Burst Duration
PRF	Pulse-Repetition Frequency
DC	Duty Cycle
SD	Sonication Duration
ISI	Inter-Stimulus Interval
AI	Acoustic Intensity
FF	Fundamental Frequency
$\mathbf{I_{sppa}}$	Spatial-Peak Pulse-Average Intensity
$\mathbf{I_{spta}}$	Spatial-Peak Temporal-Average Intensity
$\mathbf{E_{sppa}}$	Energy Density
FWHM	Full-Width-at-Half-Maximum

References

1. Ettinger GJ, Leventon ME, Grimson WE, Kikinis R, Gugino L, Cote W, et al. Experimentation with a transcranial magnetic stimulation system for functional brain mapping. Medical image analysis. 1998 Jun; 2(2):133–142. [Research Support, Non-U.S. Gov't Research Support, U.S. Gov't, Non-P.H.S.]. [PubMed: 10646759]
2. Picht T, Schmidt S, Brandt S, Frey D, Hannula H, Neuvonen T, et al. Preoperative functional mapping for rolandic brain tumor surgery: comparison of navigated transcranial magnetic stimulation to direct cortical stimulation. Neurosurgery. 2011 Sep; 69(3):581–588. [Comparative Study]. [PubMed: 21430587]
3. Mancuso JJ, Kim J, Lee S, Tsuda S, Chow NB, Augustine GJ. Optogenetic probing of functional brain circuitry. Experimental physiology. 2011 Jan; 96(1):26–33. [Review]. [PubMed: 21056968]
4. Lele PP. A simple method for production of trackless focal lesions with focused ultrasound: physical factors. J Physiol. 1962 Mar.160:494–512. [PubMed: 14463953]
5. McDannold NJ, Jolesz FA, Hynynen KH. Determination of the Optimal Delay between Sonications during Focused Ultrasound Surgery in Rabbits by Using MR Imaging to Monitor Thermal Buildup in Vivo1. Radiology. 1999; 211(2):419–426. [PubMed: 10228523]
6. Clement GT, White PJ, King RL, McDannold N, Hynynen K. A magnetic resonance imaging-compatible, large-scale array for trans-skull ultrasound surgery and therapy. J Ultrasound Med. 2005 Aug; 24(8):1117–1125. [In Vitro Research Support, N.I.H., Extramural Research Support, Non-U.S. Gov't Research Support, U.S. Gov't, P.H.S.]. [PubMed: 16040827]
7. Hynynen K, Jolesz FA. Demonstration of Potential Noninvasive Ultrasound Brain Therapy Through an Intact Skull. Ultrasound in medicine & biology. 1998; 24(2):275–283. [PubMed: 9550186]
8. White PJ, Clement GT, Hynynen K. Longitudinal and shear mode ultrasound propagation in human skull bone. Ultrasound Med Biol. 2006 Jul; 32(7):1085–1096. [Research Support, N.I.H., Extramural]. [PubMed: 16829322]
9. Fry FJ, Ades HW, Fry WJ. Production of reversible changes in the central nervous system by ultrasound. Science. 1958 Jan 10; 127(3289):83–84. [PubMed: 13495483]
10. Manlapaz JS, Astroem KE, Ballantine HT Jr, Lele PP. Effects of Ultrasonic Radiation in Experimental Focal Epilepsy in the Cat. Experimental neurology. 1964 Oct.10:345–356. [PubMed: 14211931]
11. Bachtold MR, Rinaldi PC, Jones JP, Reines F, Price LR. Focused ultrasound modifications of neural circuit activity in a mammalian brain. Ultrasound Med Biol. 1998 May; 24(4):557–565. [In Vitro Research Support, Non-U.S. Gov't]. [PubMed: 9651965]
12. Rinaldi PC, Jones JP, Reines F, Price LR. Modification by focused ultrasound pulses of electrically evoked responses from an in vitro hippocampal preparation. Brain research. 1991 Aug 30; 558(1): 36–42. [In Vitro Research Support, Non-U.S. Gov't]. [PubMed: 1933382]
13. Min BK, Bystritsky A, Jung KI, Fischer K, Zhang Y, Maeng LS, et al. Focused ultrasound-mediated suppression of chemically-induced acute epileptic EEG activity. BMC Neurosci. 2011; 12:23. [PubMed: 21375781]
14. Yoo SS, Bystritsky A, Lee JH, Zhang Y, Fischer K, Min BK, et al. Focused ultrasound modulates region-specific brain activity. Neuroimage. 2011 Jun 1; 56(3):1267–1275. [PubMed: 21354315]
15. Kim H, Taghados SJ, Fischer K, Maeng LS, Park S, Yoo SS. Noninvasive Transcranial Stimulation of Rat Abducens Nerve by Focused Ultrasound. Ultrasound Med Biol. 2012 Sep; 38(9):1568–1575. [PubMed: 22763009]
16. Bystritsky A, Korb AS, Douglas PK, Cohen MS, Melega WP, Mulgaonkar AP, et al. A review of low-intensity focused ultrasound pulsation. Brain Stimul. 2011 Jul; 4(3):125–136. [PubMed: 21777872]
17. Tufail Y, Yoshihiro A, Pati S, Li MM, Tyler WJ. Ultrasonic neuromodulation by brain stimulation with transcranial ultrasound. Nature protocols. 2011 Sep; 6(9):1453–1470. [Research Support, Non-U.S. Gov't Research Support, U.S. Gov't, Non-P.H.S.].
18. Tufail Y, Matyushov A, Baldwin N, Tauchmann ML, Georges J, Yoshihiro A, et al. Transcranial Pulsed Ultrasound Stimulates Intact Brain Circuits. Neuron. 2010 Jul 10; 66(5):681–694. [PubMed: 20547127]

19. Harvey EN. The effect of high frequency sound waves on heart muscle and other irritable tissues. American Journal of Physiology -- Legacy Content. 1929 Dec 1; 91(1):284–290. 1929.
20. Tsui PH, Wang SH, Huang CC. In vitro effects of ultrasound with different energies on the conduction properties of neural tissue. Ultrasonics. 2005 Jun; 43(7):560–565. [Research Support, Non-U.S. Gov't]. [PubMed: 15950031]
21. Foley JL, Little JW, Vaezy S. Image-guided high-intensity focused ultrasound for conduction block of peripheral nerves. Annals of biomedical engineering. 2007 Jan; 35(1):109–119. [Research Support, Non-U.S. Gov't Research Support, U.S. Gov't, Non-P.H.S.]. [PubMed: 17072498]
22. Karshafian R, Bevan PD, Williams R, Samac S, Burns PN. Sonoporation by ultrasound-activated microbubble contrast agents: effect of acoustic exposure parameters on cell membrane permeability and cell viability. Ultrasound Med Biol. 2009 May; 35(5):847–860. [Research Support, Non-U.S. Gov't]. [PubMed: 19110370]
23. King RL, Brown JR, Newsome WT, Pauly KB. Effective parameters for ultrasound-induced in vivo neurostimulation. Ultrasound Med Biol. 2013 Feb; 39(2):312–331. [Research Support, Non-U.S. Gov't]. [PubMed: 23219040]
24. NEMA. Acoustic Output Measurement Standard for Diagnostic Ultrasound Equipment. Washinton, DC: National Electrical Manufactures Association; 2004.
25. Bercoff J, Tanter M, Fink M. Supersonic shear imaging: a new technique for soft tissue elasticity mapping. IEEE Trans Ultrason Ferroelectr Freq Control. 2004 Apr; 51(4):396–409. [PubMed: 15139541]
26. Younan Y, Deffieux T, Larrat B, Fink M, Tanter M, Aubry JF. Influence of the pressure field distribution in transcranial ultrasonic neurostimulation. Med Phys. 2013 Aug.40(8):082902. [Research Support, Non-U.S. Gov't]. [PubMed: 23927357]
27. Mehic E, Xu JM, Caler CJ, Coulson NK, Moritz CT, Mourad PD. Increased anatomical specificity of neuromodulation via modulated focused ultrasound. PLoS One. 2014; 9(2):e86939. [PubMed: 24504255]
28. Yoo SS, Kim H, Min BK, Franck E, Park S. Transcranial focused ultrasound to the thalamus alters anesthesia time in rats. Neuroreport. 2011 Oct 26; 22(15):783–787. [PubMed: 21876461]
29. Kim H, Chiu A, Park S, Yoo S-S. Image-guided navigation of single-element focused ultrasound transducer. International Journal of Imaging Systems and Technology. 2012; 22(3):177–184. [10.1002/ima.22020].
30. Fonoff ET, Pereira JF Jr, Camargo LV, Dale CS, Pagano RL, Ballester G, et al. Functional mapping of the motor cortex of the rat using transdural electrical stimulation. Behavioural Brain Research. 2009; 202(1):138–141. [PubMed: 19447290]
31. Min B-K, Yang PS, Bohlke M, Park S, Rvago D, Maher TJ, et al. Focused ultrasound modulates the level of cortical neurotransmitters: Potential as a new functional brain mapping technique. International Journal of Imaging Systems and Technology. 2011; 21(2):232–240. [10.1002/ima.20284].
32. O'Brien WD Jr. Ultrasound-biophysics mechanisms. Prog Biophys Mol Biol. 2007 Jan-Apr;93(1–3):212–255. [Research Support, N.I.H., Extramural Review]. [PubMed: 16934858]
33. Wahab RA, Choi M, Liu Y, Krauthamer V, Zderic V, Myers MR. Mechanical bioeffects of pulsed high intensity focused ultrasound on a simple neural model. Med Phys. 2012 Jul; 39(7):4274–4283. [PubMed: 22830761]
34. Duck FA. Medical and non-medical protection standards for ultrasound and infrasound. Prog Biophys Mol Biol. 2007 Jan-Apr;93(1–3):176–191. [PubMed: 16965806]
35. Plaksin M, Shoham S, Kimmel E. Intramembrane Cavitation as a Predictive Bio-Piezoelectric Mechanism for Ultrasonic Brain Stimulation. Phys Rev X. 2014; 4(1):011004. [10.1103/PhysRevX.4.011004].
36. Ascoli GA, Alonso-Nanclares L, Anderson SA, Barrionuevo G, Benavides-Piccione R, et al. Petilla Interneuron Nomenclature G. Petilla terminology: nomenclature of features of GABAergic interneurons of the cerebral cortex. Nature reviews Neuroscience. 2008 Jul; 9(7):557–568.
37. Dalecki D. Mechanical bioeffects of ultrasound. Annual review of biomedical engineering. 2004; 6:229–248. [Research Support, U.S. Gov't, P.H.S. Review].

38. Fix AS, Ross JF, Stitzel SR, Switzer RC. Integrated evaluation of central nervous system lesions: stains for neurons, astrocytes, and microglia reveal the spatial and temporal features of MK-801-induced neuronal necrosis in the rat cerebral cortex. Toxicologic pathology. 1996 May-Jun;24(3): 291–304. [PubMed: 8736385]

Highlights

- The ‘sweet-spot’ in excitatory neuromodulation of pulsed FUS was identified.
- 1–5ms TBD, 50% DC, 300ms SD stimulates the somatomotor area at the lowest AIs.
- The use of 350 kHz fundamental frequency outperforms 650 kHz.
- The pulsed FUS outperforms the equivalent continuous sonication.

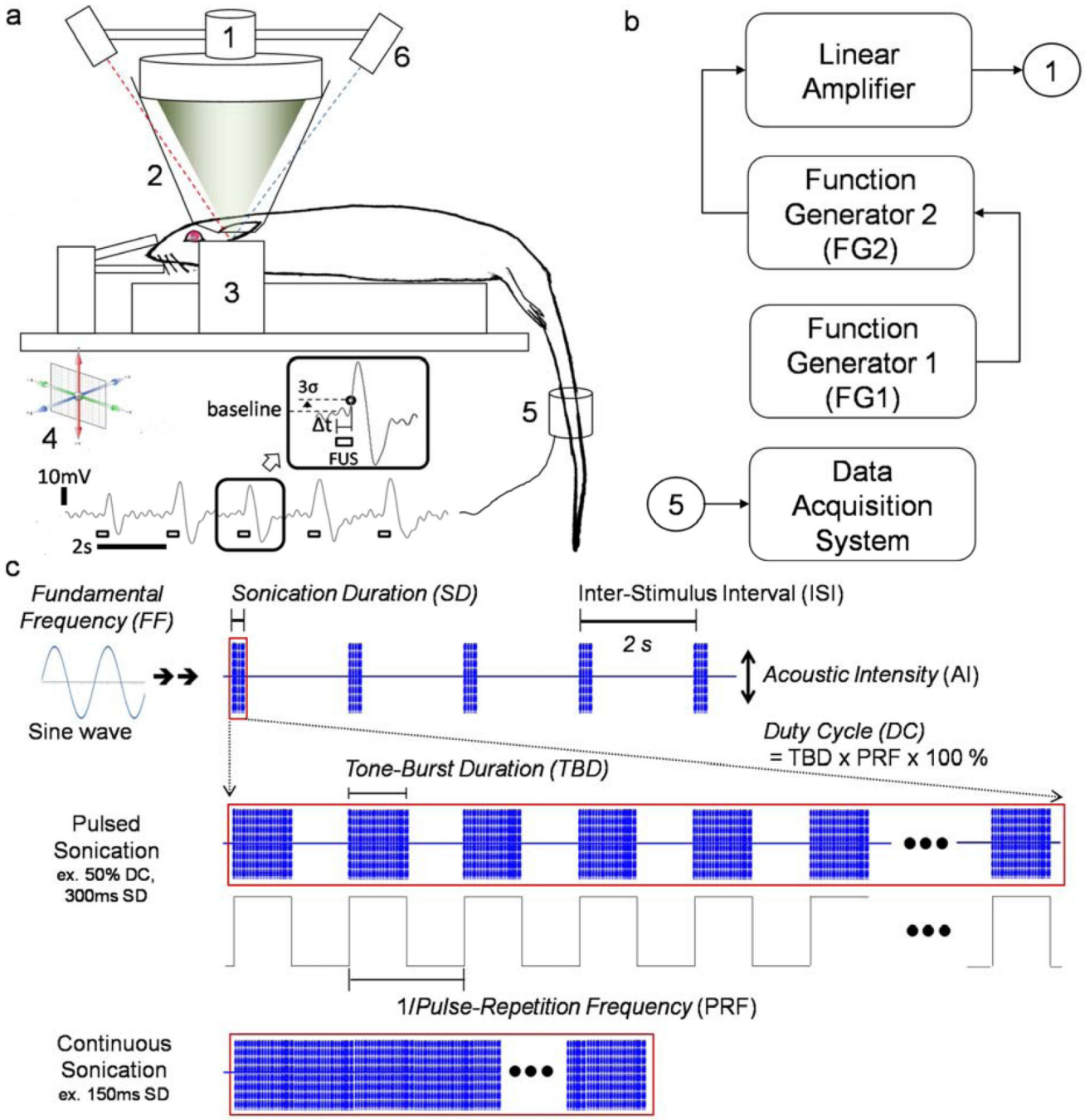

Figure 1.

(a) Experimental set-up to test excitatory neuromodulation (tail movement) using focused ultrasound in rat: (1) single-element FUS transducer, (2) degassed water bag, (3) rat fixation frame, (4) 3-axes adjustable platform, (5) motion detection sensor, (6) optical-guidance system (dashed lines represent visible lasers); an exemplar record of the induced tail movement by pulsed FUS (350 kHz FF, 50% DC – 250 Hz PRF, 2ms TBD, 300ms SD, 2s ISI) as an inset; we used 3 times the standard deviation (denoted as 'σ') of the baseline signal level as the threshold to estimate the response latency from the onset of stimulation,

(b) Schematics of sonication control and acquisition system, (c) Definition of sonication parameters modulated by function generators (FGs): tone-burst duration (TBD), pulse-repetition frequency (PRF), duty cycle (DC), sonication duration (SD), inter-stimulus interval (ISI), acoustic intensity (AI), and fundamental frequency (FF).

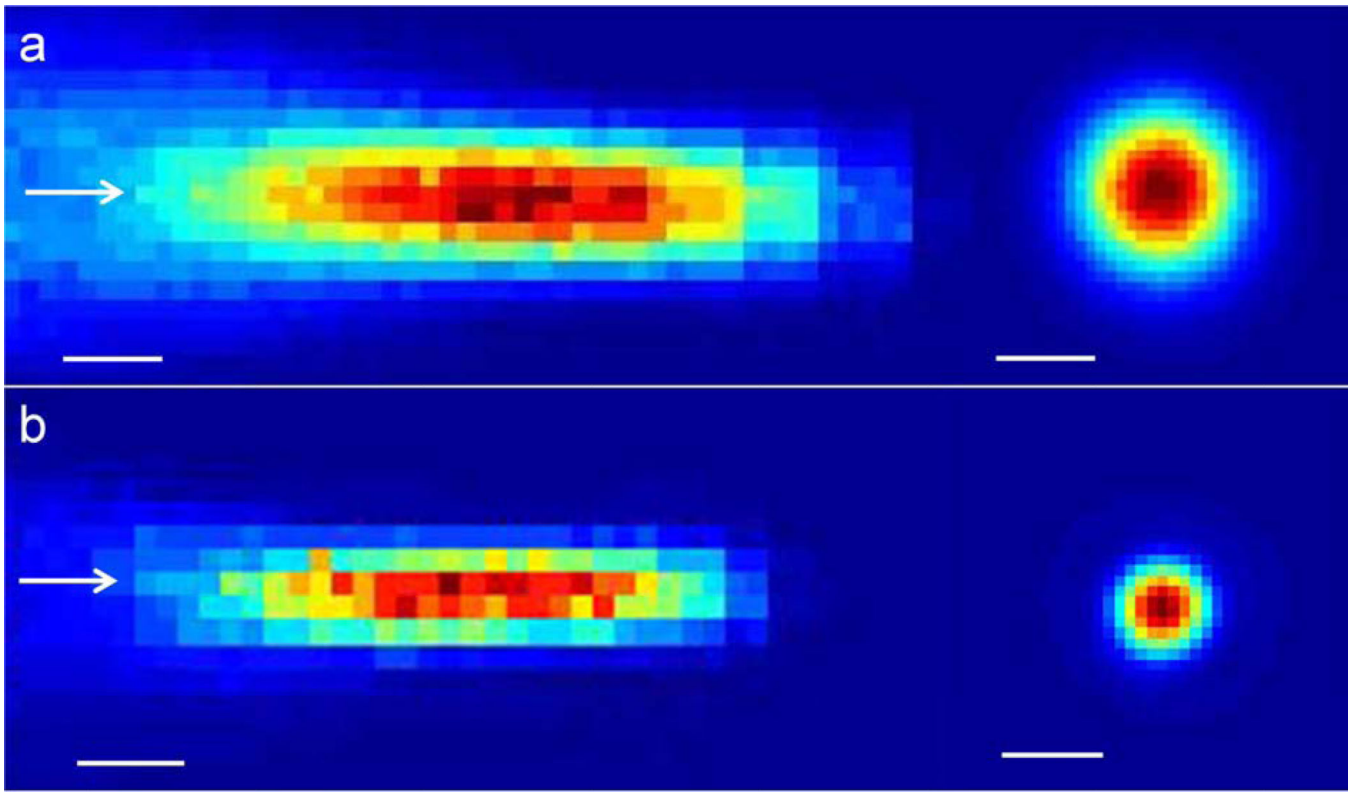

Figure 2.

Acoustic intensity profile of (a) 350 kHz and (b) 650 kHz transducer in longitudinal (left) and transversal (right) plane to the sonication path. The arrows indicate the direction of sonication. The bars indicate the 5 mm scale.

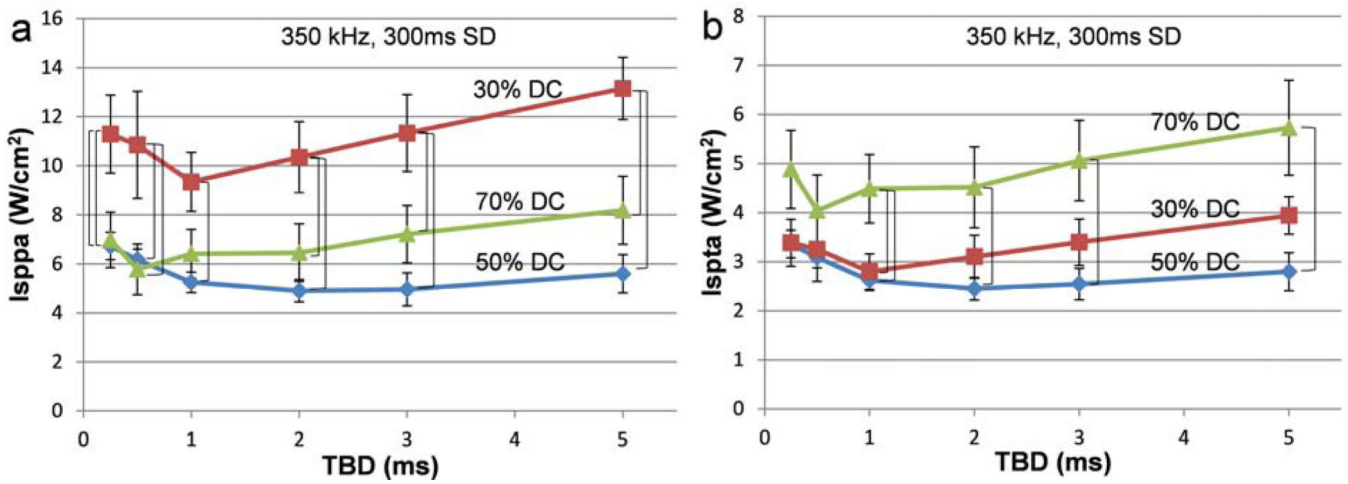

Figure 3.

Comparison of threshold acoustic intensities among the three duty cycles across the six tone-burst durations. For the fixed fundamental frequency (350 kHz) and sonication duration (300 ms), the association of the threshold (a) I_{sppa} and (b) I_{spta} to the three different duty cycles across various tone-burst durations is shown. The brackets indicate statistically significant differences (one-way ANOVA with Tukey-Kramer *post-hoc* analysis; $p<0.05$) at the specified TBD. The error bars indicate ±1 s.e.m.

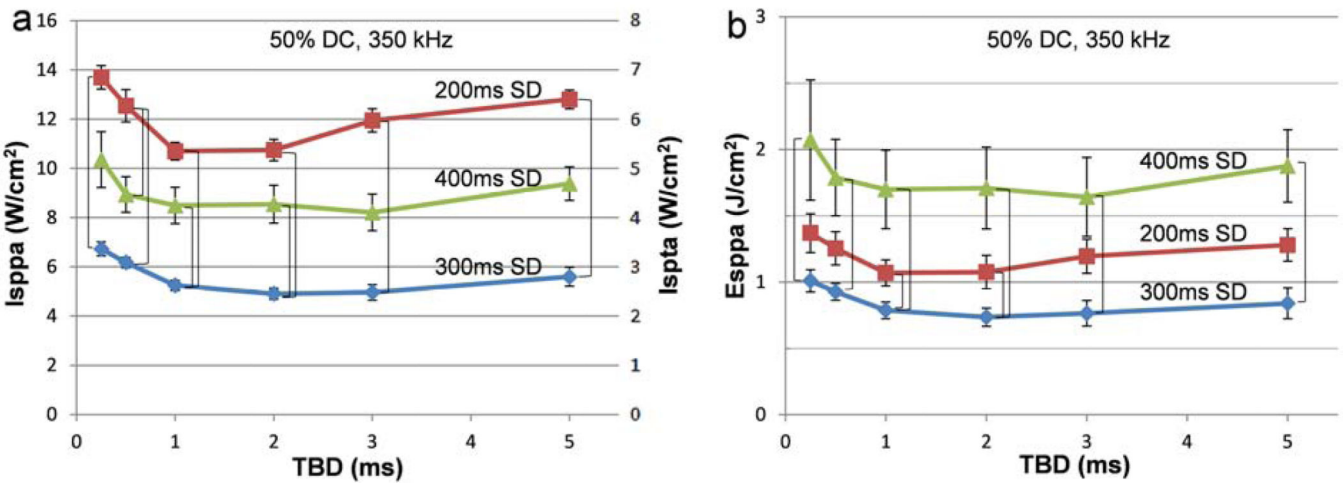

Figure 4.

Comparison of threshold acoustic intensities and energy density among the three sonication durations across the six tone-burst durations. For the fixed duty cycle (50%) and fundamental frequency (350 kHz), the association of the threshold (a) AIs (I_{sppa} and I_{spta}) and (b) E_{sppa} to the three different sonication durations across various tone-burst durations is shown. The brackets indicate statistically significant differences (one-way ANOVA with Tukey-Kramer *post-hoc* analysis; $p<0.05$) at the specified TBD. The error bars (I_{sppa} and E_{sppa}) indicate ±1 s.e.m.

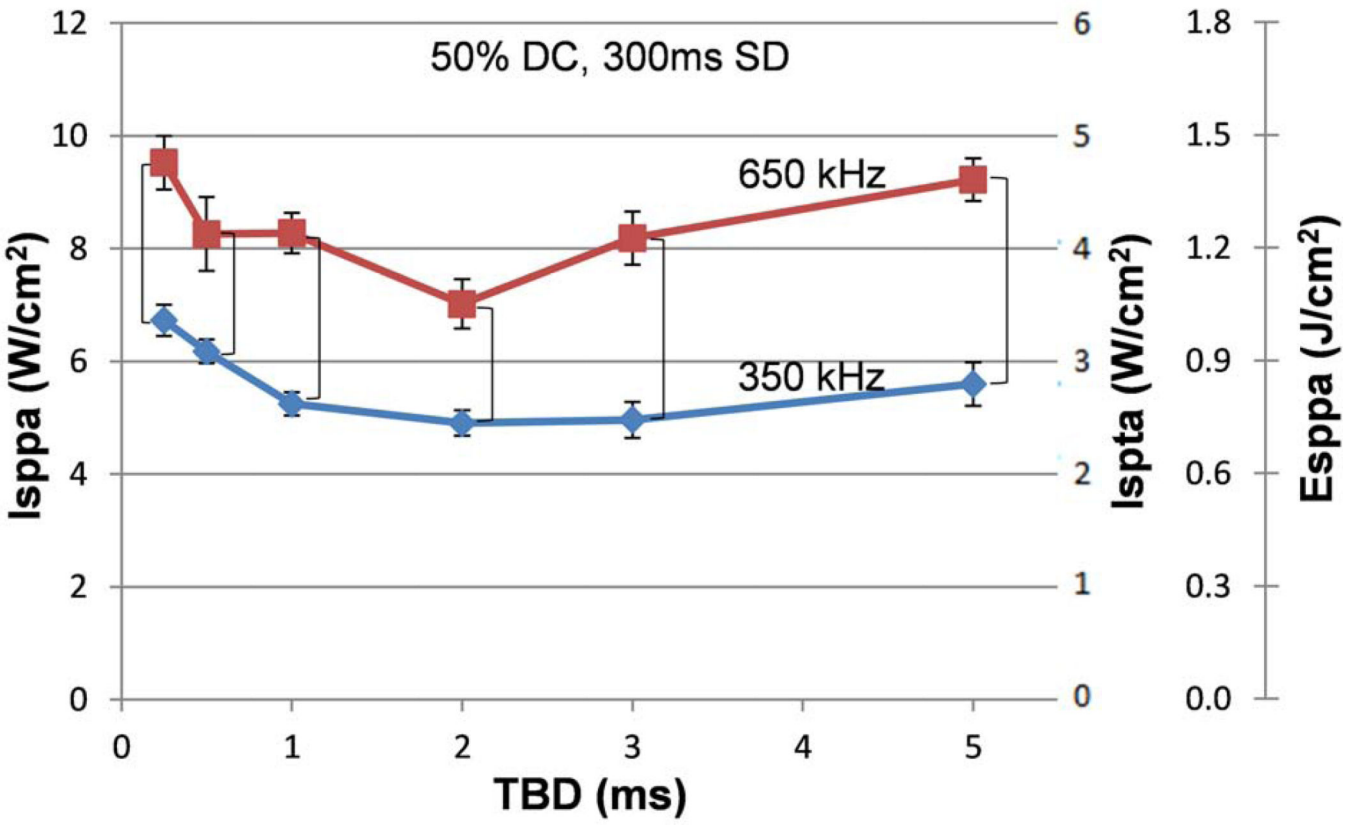

Figure 5.

Comparison of threshold acoustic intensities and energy density between the two fundamental frequencies across the six tone-burst durations. For the fixed duty cycle (50%) and sonication duration (300 ms), the association of threshold AIs (I_{sppa} and I_{spta}) and E_{sppa} to the two different fundamental frequencies at various tone-burst durations is shown. The brackets indicate statistically significant differences (one-tailed t-test; $p<0.05$) at the specified TBD. The error bars (I_{sppa} only) indicate ±1 s.e.m. It can be seen that the use of 350 kHz could elicit motor responses at lower threshold acoustic intensities.

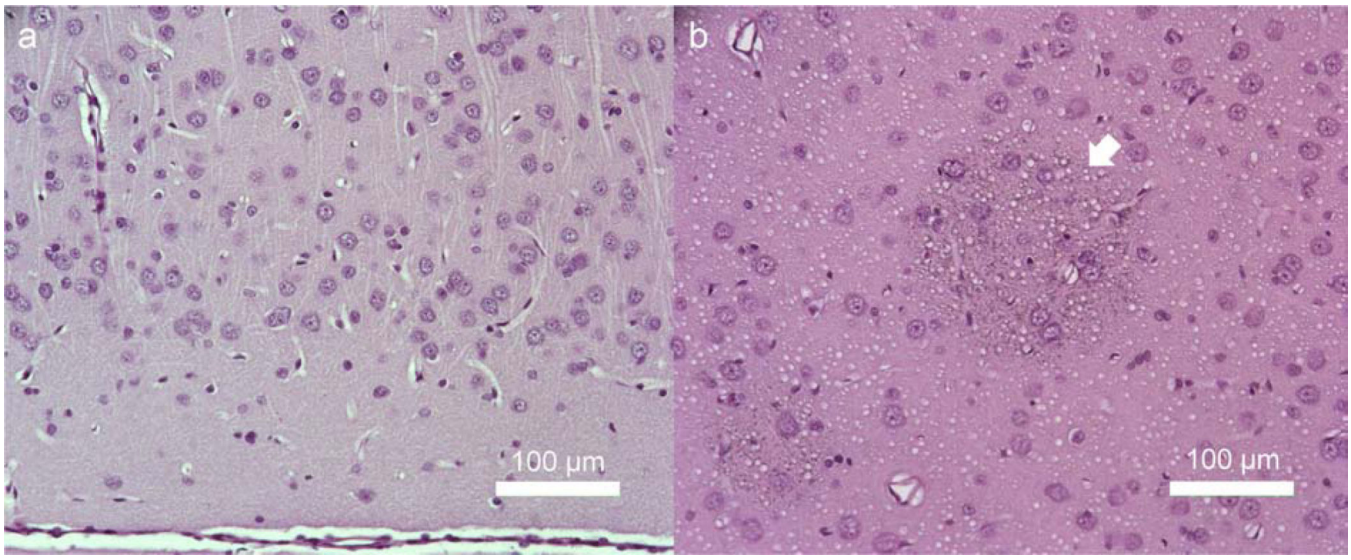

Figure 6.

Examples of the histological analysis of the sonicated rat brain tissues. (a) Hematoxylin and eosin (H&E) staining confirmed that there was no tissue damage or hemorrhage associated with the sonication in a majority of the animals (n=29 out of 30). (b) Tissue sample from the one animal, whereby several rounded shapes containing hemosiderin were observed. The animal was allowed to survive for 26 days after the sonication before being sacrificed. Several rounded areas containing hemosiderin indicating potential earlier bleeding was observed (shown in arrow). Both sections were sampled from the brain cortex near the mid-line.

Table 1

Combination of sonication parameters used in this study.

Frequency (kHz)	DC (%)	TBD (ms)	PRF (kHz)	SD (ms)
350	50	0.25	2.00	300
350	50	0.5	1.00	300
350	50	1	0.50	300
350	50	2	0.25	300
350	50	3	0.17	300
350	50	5	0.10	300
350	30	0.25	1.20	300
350	30	0.5	0.60	300
350	30	1	0.30	300
350	30	2	0.15	300
350	30	3	0.10	300
350	30	5	0.06	300
350	70	0.25	2.80	300
350	70	0.5	1.40	300
350	70	1	0.70	300
350	70	2	0.35	300
350	70	3	0.23	300
350	70	5	0.14	300
350	50	0.25	2.00	200
350	50	0.5	1.00	200
350	50	1	0.50	200
350	50	2	0.25	200
350	50	3	0.17	200
350	50	5	0.10	200
350	50	0.25	2.00	400
350	50	0.5	1.00	400
350	50	1	0.50	400
350	50	2	0.25	400
350	50	3	0.17	400
350	50	5	0.10	400
650	50	0.5	1.00	300
650	50	1	0.50	300
650	50	2	0.25	300
650	50	3	0.17	300
650	50	5	0.10	300
350	100	-	-	150

Table 2

One-way ANOVA and t-test (two-tailed) results of the group difference in animal weight. The abbreviations are as follows (H_0: null hypothesis, μ: population mean, df: degree-of-freedom, F: F-value, t: t-value, and p: p-value).

		Animal Weight			
	H_0	**df**	**F**	**t**	**p**
DC (%)	$\mu^{30}=\mu^{50}=\mu^{70}$	2,27	0.46		0.64
SD (ms)	$\mu^{200}=\mu^{300}=\mu^{400}$	2,26	1.06		0.36
FF (kHz)	$\mu^{350}=\mu^{650}$	17		−1.05	0.31
Mode	$\mu^{pulsed}=\mu^{continuous}$	18		−2.05	0.06